



Missouri University of Science and Technology
Scholars' Mine

International Specialty Conference on Cold-Formed Steel Structures

(1975) - 3rd International Specialty Conference on Cold-Formed Steel Structures

Nov 24th, 12:00 AM

Cold-forming Residual Stresses Effect on Buckling

Lars Ingvarsson

Follow this and additional works at: <https://scholarsmine.mst.edu/isccss>

 Part of the [Structural Engineering Commons](#)

Recommended Citation

Ingvarsson, Lars, "Cold-forming Residual Stresses Effect on Buckling" (1975). *International Specialty Conference on Cold-Formed Steel Structures*. 4.

<https://scholarsmine.mst.edu/isccss/3iccfss/3iccfss-session1/4>

This Article - Conference proceedings is brought to you for free and open access by Scholars' Mine. It has been accepted for inclusion in International Specialty Conference on Cold-Formed Steel Structures by an authorized administrator of Scholars' Mine. This work is protected by U. S. Copyright Law. Unauthorized use including reproduction for redistribution requires the permission of the copyright holder. For more information, please contact scholarsmine@mst.edu.

COLD-FORMING RESIDUAL STRESSES. EFFECT ON BUCKLING

by Lars Ingvarsson^{x)}

1. INTRODUCTION

This work is a part of an investigation at The Dept. of Building Statics and Structural Engineering, Royal Institute of Technology, Stockholm, concerning welded box columns with regard to mode of action and constructional suitability. Particularly the possibility of using quenched and tempered steel (yield stress about 700 N/mm^2) in box columns built up by two thick channel-sections welded together is studied.

Very interesting results have been obtained. Both theoretical and experimental stress analysis indicates that there are residual stresses due to cold-forming not only in the circumferential direction but also in the length direction of channel members. Results from residual stress measurements and an analytic study according to the theory of plasticity are presented herein.

By using a method of calculation for plate buckling in the overcritical range, developed by Professor *H Nylander*^{xx)}/6/, it has been possible in

x) Lars Ingvarsson is Research Assistant at The Dept. of Building Statics and Structural Engineering, The Royal Institute of Technology, Stockholm, Sweden.

xx) Henrik Nylander is Professor and Head of The Dept. of Building Statics and Structural Engineering, The Royal Institute of Technology, Stockholm, Sweden.

a relatively simple manner to consider residual stresses due to cold-forming and welding in combination with initial deflections. The method of calculation and theoretical results are presented. Results from buckling tests carried out at the department by the author are also enclosed.

2. RESIDUAL STRESSES DUE TO COLD-FORMING

2.1 Analytical study

2.11 Idealized case

An idealized case will be treated in order to explain the phenomenon of residual stresses in the length direction of a cold-formed member. A polar coordinate system illustrated in FIGURE 1 is used, where ρ is an internal radial coordinate beginning at the inner surface.

$$\rho = r - r_i \quad (1)$$

where

r_i = inner radius, which is varied during the cold-forming.

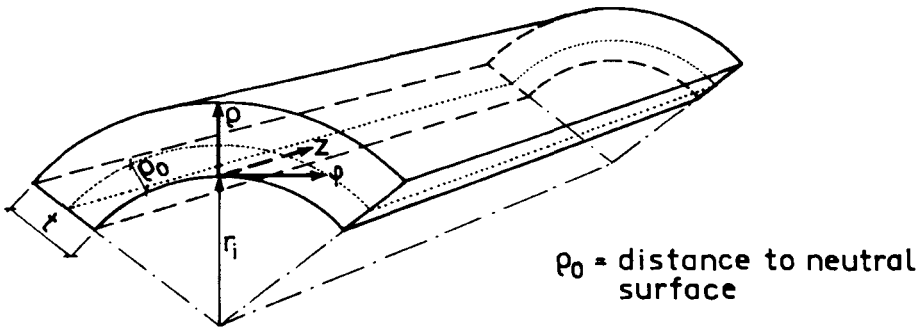


FIGURE 1 Coordinate system.

The mechanism of cold-forming involves two basic events. A flat plate is plastically deformed by external forces followed by an elastic unloading. In order to simplify the treatment, polar symmetrical loading forces are assumed. They are illustrated in FIGURE 2 where m_φ = bending moment, n_φ = circumferential normal force and σ_{ri} = radial pressure at the inner surface.

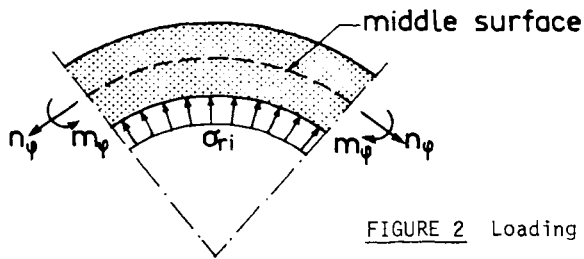


FIGURE 2 Loading forces.

2.12 General relations

Because of the symmetrical loading the principal stress and strain directions are equal to the polar coordinate axis. By using the distortion energy theory (*von Mises* /5/) the yield criterion can be written

$$\sigma_e = \frac{1}{\sqrt{2}} \left[(\sigma_\varphi - \sigma_r)^2 + (\sigma_r - \sigma_z)^2 + (\sigma_z - \sigma_\varphi)^2 \right]^{1/2} \geq \sigma_y \quad (1)$$

where

σ_e = equivalent stress and σ_φ , σ_r , σ_z = stresses in the polar coordinate directions and σ_y = yield stress at uniaxial test.

The increments of strain consist of one elastic and one plastic part, which gives (referring to *Mendelson* /4/)

$$\begin{cases} d\epsilon_{\varphi} = d\epsilon_{\varphi}^e + d\epsilon_{\varphi}^p & (3a) \\ d\epsilon_r = d\epsilon_r^e + d\epsilon_r^p & (3b) \\ d\epsilon_z = d\epsilon_z^e + d\epsilon_z^p & (3c) \end{cases}$$

where

$d\epsilon_{\varphi}, d\epsilon_r, d\epsilon_z$ = total strain increments,
 $d\epsilon_{\varphi}^e, d\epsilon_r^e, d\epsilon_z^e$ = elastic strain increments,
 and $d\epsilon_{\varphi}^p, d\epsilon_r^p, d\epsilon_z^p$ = plastic strain increments.

By using *Prandtl-Reuss* Equations (/7/, /8/), based on the *von Mises* criterion, the expressions for the plastic strain increments will be

$$\begin{cases} d\epsilon_{\varphi}^p = \frac{d\epsilon_p^p}{\sigma_e} \left[\sigma_{\varphi} - \frac{1}{2} (\sigma_r + \sigma_z) \right] & (4a) \end{cases}$$

$$\begin{cases} d\epsilon_r^p = \frac{d\epsilon_p^p}{\sigma_e} \left[\sigma_r - \frac{1}{2} (\sigma_z + \sigma_{\varphi}) \right] & (4b) \end{cases}$$

$$\begin{cases} d\epsilon_z^p = \frac{d\epsilon_p^p}{\sigma_e} \left[\sigma_z - \frac{1}{2} (\sigma_{\varphi} + \sigma_r) \right] & (4c) \end{cases}$$

where

$$d\epsilon_p = \frac{\sqrt{2}}{3} \left[(d\epsilon_{\varphi}^p - d\epsilon_r^p)^2 + (d\epsilon_r^p - d\epsilon_z^p)^2 + (d\epsilon_z^p - d\epsilon_{\varphi}^p)^2 \right]^{\frac{1}{2}} \quad (5)$$

is the equivalent plastic strain increment.

The elastic strain increments are given by differentiation of *Hooke's* generalized law

$$\begin{cases} d\epsilon_{\varphi}^e = \frac{1}{E} \left[d\sigma_{\varphi} - \nu(d\sigma_r + d\sigma_z) \right] & (6a) \end{cases}$$

$$\begin{cases} d\epsilon_r^e = \frac{1}{E} \left[d\sigma_r - \nu(d\sigma_z + d\sigma_{\varphi}) \right] & (6b) \end{cases}$$

$$\begin{cases} d\epsilon_z^e = \frac{1}{E} \left[d\sigma_z - \nu(d\sigma_{\varphi} + d\sigma_r) \right] & (6c) \end{cases}$$

where E is the modulus of elasticity and ν is *Poisson's* ratio.

2.13 Equilibrium relation

With polar coordinates and axial symmetry the equilibrium equation becomes

$$\frac{d\sigma_r}{dr} - \frac{1}{r} (\sigma_\varphi - \sigma_r) = 0 \quad (7)$$

which gives

$$\sigma_r = \int \frac{1}{r} (\sigma_\varphi - \sigma_r) dr \quad (7)$$

A boundary condition is

$$\sigma_r(r_{\text{out}}) = 0 \quad (8)$$

where r_{out} is the radius of the outer surface.

Substituting (1), (8) into (7) and introducing the curvature of the inner surface

$$C = 1/r_i \quad (9)$$

gives the evaluated equilibrium equation

$$\sigma_r = \int_{\rho_{\text{out}}}^{\rho} \frac{C}{1+\rho C} (\sigma_r - \sigma_\varphi) d\rho \quad (10)$$

2.14 Geometrical relations

The geometrical relations are studied in FIGURE 3. Assuming plane sections to remain plane gives

$$\epsilon_\varphi = \frac{r d\varphi - r_0 d\varphi}{r_0 d\varphi} = C_0 (\rho - \rho_0) \quad (11)$$

where $C_0 = 1/r_0$ is the curvature of the neutral surface

$$C_o = \frac{1}{\rho_o + r_i} = \frac{C}{1 + \rho_o C} \quad (12)$$

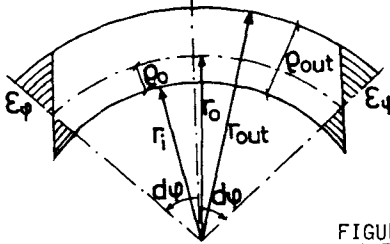


FIGURE 3 Geometry.

Differentiation of (11) and (12) gives an evaluated geometric relation for the circumferential strain increment

$$d\varepsilon_\phi = \frac{\rho - \rho_o}{(1 + \rho_o C)^2} dC \quad (13)$$

where dC is the curvature increment of the inner surface.

A basic assumption in this treatment is made for the strain increment in the length direction.

$$d\varepsilon_z = 0 \quad (14)$$

which is accurate if the ends of a cold-formed member are fixed. This can be assumed because of the friction in used press brakes. A discussion of this assumption will be made below in chapter 2.18.

2.15 Stress-strain relations

Of interest is the relation between plastic and elastic strains. There are three phases.

Phase (I) : ELASTIC behaviour

$$\begin{cases} d\epsilon_p = 0 \\ \sigma_e < \sigma_y \end{cases} \quad (15a)$$

where σ_y = yield stress at uniaxial tensile test

Phase (II) : PLASTIC behaviour

The yield criterion of *von Mises* /5/ gives

$$\begin{cases} \sigma_e = \sigma_y \\ d\epsilon_p \neq 0 \end{cases}$$

Assuming $d\epsilon_\varphi = d\epsilon_\varphi^p$

substituted into (4a) gives

$$d\epsilon_p = d\epsilon_\varphi \cdot \sigma_y / \left[\sigma_\varphi - \frac{1}{2}(\sigma_r + \sigma_z) \right] \quad (15b)$$

Phase (III) : STRAIN-HARDENING

One can define an equivalent total strain by

$$\epsilon_{et} = \frac{\sqrt{2}}{3} \left[(\epsilon_\varphi - \epsilon_r)^2 + (\epsilon_r - \epsilon_z)^2 + (\epsilon_z - \epsilon_\varphi)^2 \right]^{\frac{1}{2}} \quad (16)$$

referring to *Mendelson* /4/, who gives the following relation using the total theory of plasticity

$$\epsilon_p = \epsilon_{et} - \frac{2}{3} \frac{(1+\nu)}{E} \sigma_e \quad (17)$$

in which ϵ_p is the equivalent plastic strain

$$\epsilon_p = \frac{\sqrt{2}}{3} \left[(\epsilon_\varphi^p - \epsilon_r^p)^2 + (\epsilon_r^p - \epsilon_z^p)^2 + (\epsilon_z^p - \epsilon_\varphi^p)^2 \right]^{\frac{1}{2}} \quad (18)$$

Differentiation of (17) gives

$$d\epsilon_p = d\epsilon_{et} - \frac{2}{3} \frac{(1+\nu)}{E} d\sigma_e$$

$$\frac{d\epsilon_p}{d\epsilon_{et}} = \frac{1}{1 + \frac{2}{3} \frac{(1+\nu)}{E} \frac{d\sigma_e}{d\epsilon_p}} \quad (19)$$

Assuming $\frac{d\epsilon_p}{d\epsilon_\varphi} = \frac{d\epsilon_p}{d\epsilon_{et}}$ substituted into (4a) gives

$$d\epsilon_p = \frac{d\epsilon_\varphi \sigma_e}{\left[\sigma_\varphi - \frac{1}{2}(\sigma_r + \sigma_z) \right] \left[1 + \frac{2}{3} \frac{d\sigma_e}{d\epsilon_p} (1+\nu)/E \right]} \quad (20)$$

Karren /2/ suggests the following convenient expression for strain-hardening

$$\begin{cases} \sigma_e = k(\epsilon_p)^n \\ k = 2.80 \sigma_u - 1.55 \sigma_y \\ n = 0.255 \sigma_u/\sigma_y - 0.120 \end{cases} \quad (21)$$

where σ_u = ultimate stress and σ_y = yield stress at uniaxial test.

Derivation gives

$$\frac{d\sigma_e}{d\epsilon_p} = nk(\epsilon_p)^{n-1} \quad (22)$$

Substituting (21), (22) into (20) gives

$$d\epsilon_p = \frac{d\epsilon_\varphi k(\epsilon_p)^n}{\left[\sigma_\varphi - \frac{1}{2}(\sigma_r + \sigma_z) \right] \left[1 + \frac{2}{3} nk(\epsilon_p)^{n-1} (1+\nu)/E \right]} \quad (15c)$$

Two types of steel will be compared. Steel "A" is an ideally elastic-plastic steel with yield stress $\sigma_y = 800 \text{ N/mm}^2$ corresponding to quenched and tempered steel. Steel "B" is a mild steel with yield stress $\sigma_y = 260 \text{ N/mm}^2$ and ultimate stress $\sigma_u = 440 \text{ N/mm}^2$. The uniaxial σ - ϵ relations of these steels are illustrated in FIGURE 4.

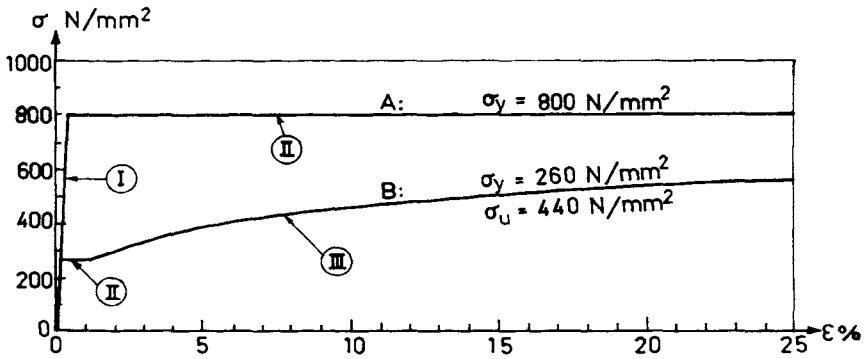


FIGURE 4 Used σ - ϵ relations in the analysis.

(I), (II), (III) shows the phases described above.

2.16 Elastic unloading

When the "active" part of the cold-forming is finished there are external forces (FIGURE 2)

$$\left\{ \begin{array}{l} m_{\varphi} = \int_0^{p_{out}} \sigma_{\varphi} (\rho - \rho_{out}/2) d\rho \end{array} \right. \quad (23)$$

$$\left\{ \begin{array}{l} n_{\varphi} = \int_0^{p_{out}} \sigma_{\varphi} d\rho \end{array} \right. \quad (24)$$

and radial pressure σ_{ri} at the inner surface. The analysis is complicated by the fact that

$$\left\{ \begin{array}{l} d\rho = (1 + \epsilon_r) dt \end{array} \right. \quad (25)$$

$$\left\{ \begin{array}{l} \rho = \int d\rho = \int (1 + \epsilon_r) dt \end{array} \right. \quad (26)$$

where dt is the thickness increment.

After the "active" cold-forming there is a springback caused by an elastic unloading of m_φ , n_φ and σ_{rj} .

The stresses of the unloading are added to those of loading. The result will be residual stresses. Of special interest is the resulting residual force per length of cold-formed arc (neutral surface).

$$n_z \text{ res} = \int_0^{\rho_{\text{out}}} \sigma_z \text{ res} (1 + \epsilon_\varphi) d\rho \quad (27)$$

The stresses caused by the elastic unloading have an exact solution, which is omitted herein. In a near future a more complete report will be published.

2.17 Incremental computer analysis

A computer program has been developed. This is described in a block diagram (FIGURE 5). The only "input-datas" are σ_y , σ_u , ρ_0/t , R_i/t where t is the initial thickness and R_i the final inner radius. Additional there are two computer parametres n_t and n_c defining

$$\left\{ \begin{array}{l} dC = 1/(R_i n_c) \end{array} \right. \quad (28)$$

$$\left\{ \begin{array}{l} dt = t/n_t \end{array} \right. \quad (29)$$

The program is built up by one outer and one inner loop. In the outer loop the curvature is changed and in the inner loop the radial position defined by ρ is changed. For each of the n_c steps increasing C , the equations mentioned above are solved for n_t radial positions between inner and outer surfaces in order to sum up the resulting stresses and strains. The central parts of the program will be run through n_t multiplied by n_c times. The program integrates stresses and strains over the "cold-forming history" by the successive increase of the curvature C .

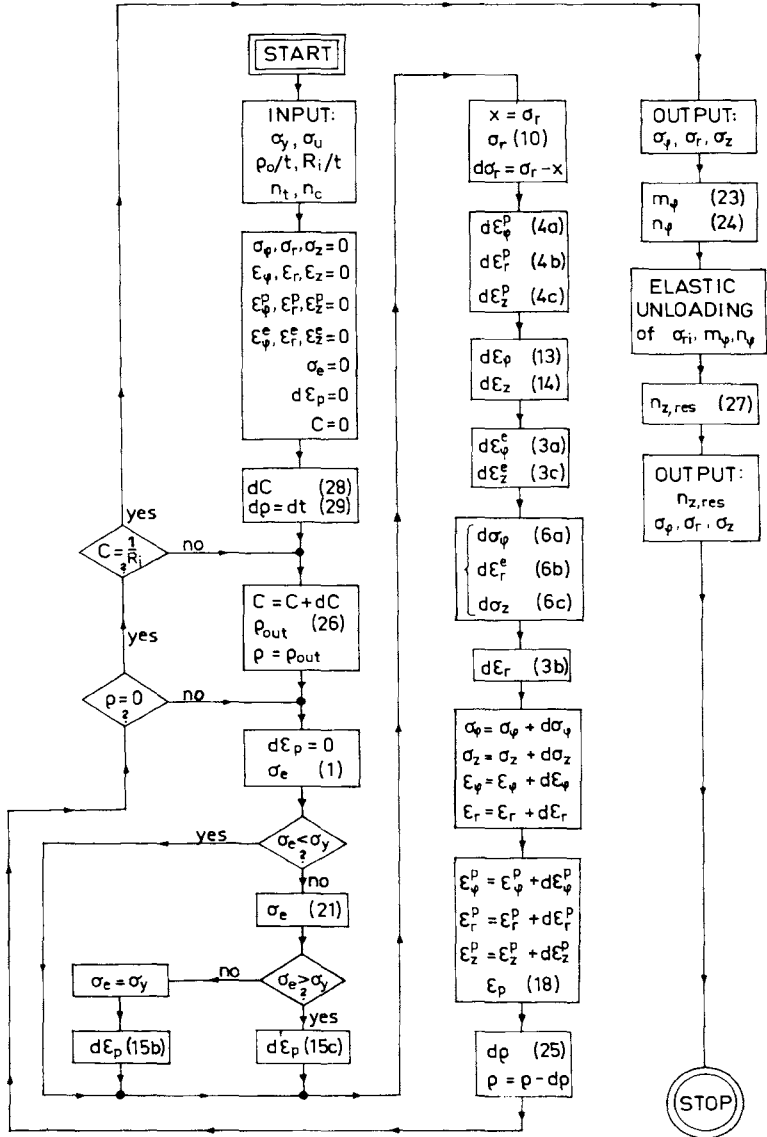


FIGURE 5 Block diagram describing computer analysis. (Numbers within brackets refers to equations in this paper.)

2.18 Corrections with regard to plane parts in cold-formed sections

The resulting residual stresses have been computed with the assumption

$$\epsilon_z = 0 \quad (14)$$

which is accurate for cold-formed members with fixed ends.

If there are no fixed ends a correction for plane parts in a cold-formed section has to be made. The request for equilibrium implies that stresses due to a reverse load $n_z \text{ res}$ must be added. For a symmetrical section the most simple correction may be written

$$\sigma_z \text{ corr} = \sigma_z \text{ res} (1 - A_c/A) \quad (28)$$

where A_c = cold-formed area and A = total area.

A more complete investigation of these problems will be published later.

2.19 Theoretical residual stresses

The computer program has been run for two types of steel presented in chapter 2.15. Examples of resulting stress-distributions before and after unloading are presented for steel A in FIGURE 6 and for steel B in FIGURE 7, where ρ_0/t are assumed to 0.25. To get enough accuracy n_t and n_c have been chosen to 100 and 1000, respectively.

Because of the three-axial stresses the circumferential stresses are higher than the yield stress after loading. Another phenomenon is the change of thickness

$$\Delta t = \rho_{\text{out}} - t \quad (29)$$

which is caused by the radial strains.

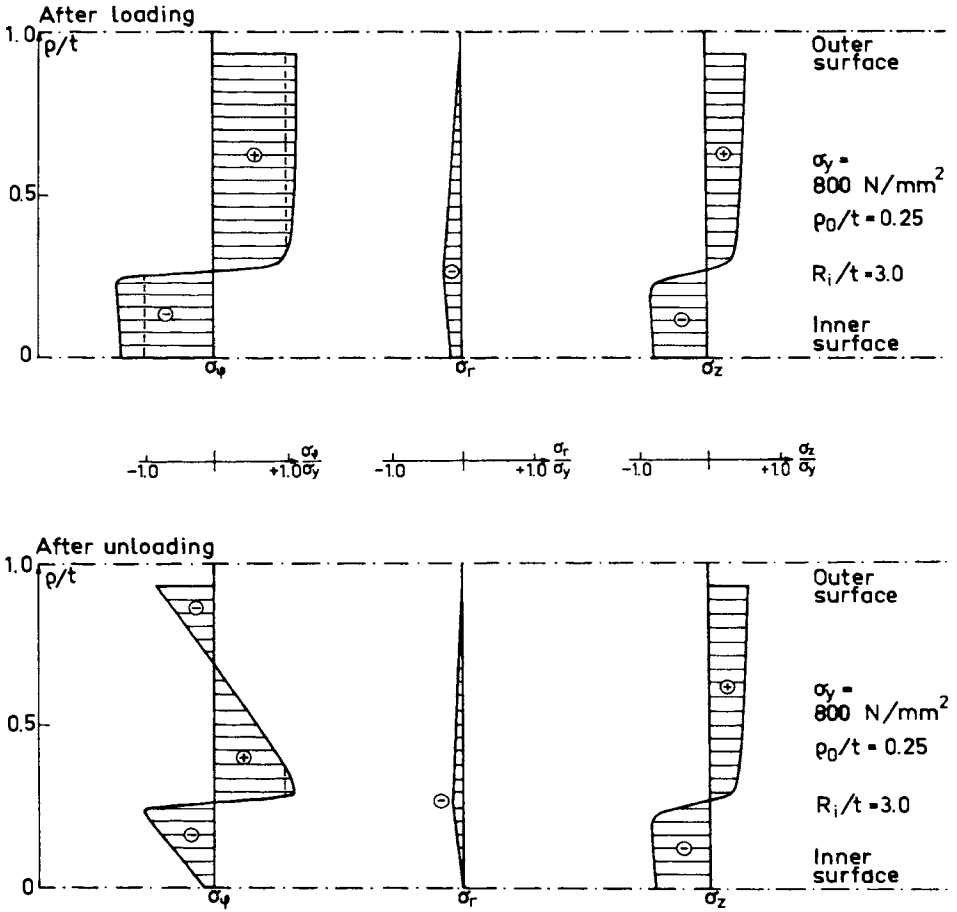


FIGURE 6 Stresses due to cold-forming. Steel A. $\rho_0/t = 0.25$. $R_i/t = 3.0$ (Ideally elastic plastic steel).

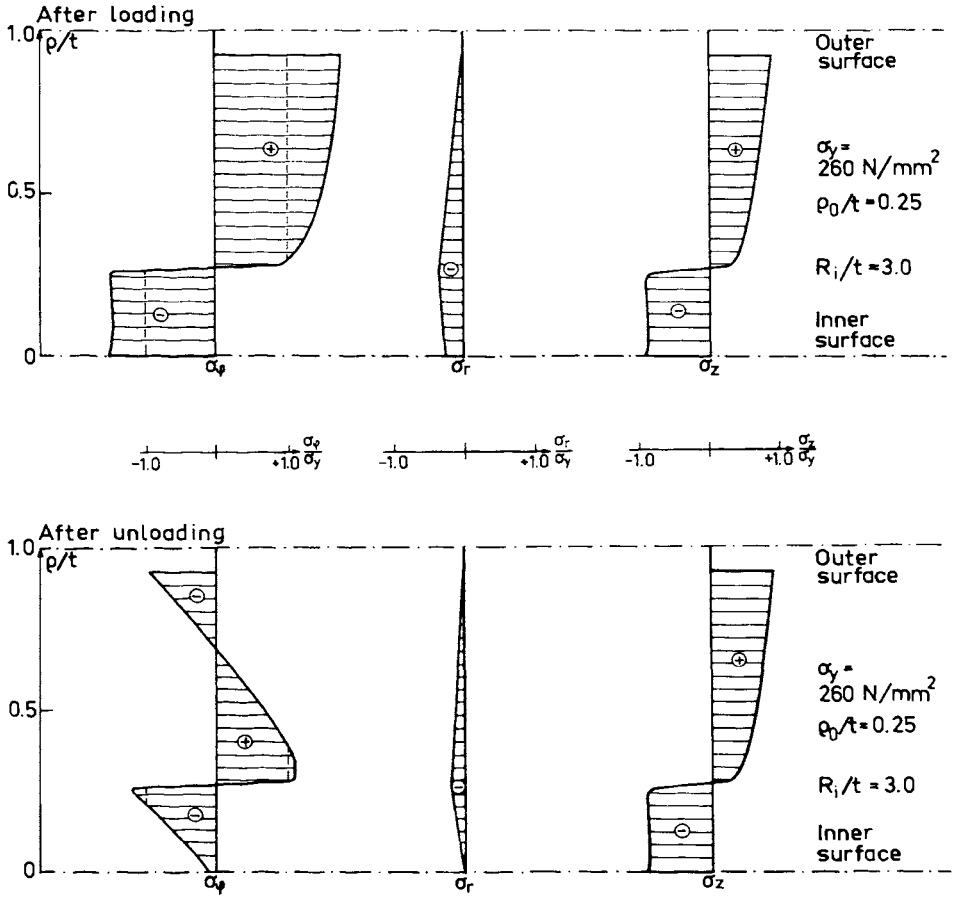


FIGURE 7 Stresses due to cold-forming. Steel B. $\rho_0/t = 0.25$. $R_i/t = 3.0$ (Strain-hardening steel).

Of great interest is the consequence of ρ_0/t , which is illustrated in FIGURES 8 and 9. In diagrams the resulting residual force $n_z \text{ res}$ and change in thickness $\Delta t/t$ are plotted as a function of ρ_0/t . With the knowledge of $\Delta t/t$ the resulting residual force $n_z \text{ res}$ can be estimated.

A remaining problem to be investigated is the influence on the ratio ρ_0/t . There are two extreme cases. If the friction at inner surface is complete (friction coefficient of 100%) the inner and the neutral surface coincide ($\rho_0/t = 0$). In this case the residual normal force and the change of thickness are maximum.

The other extreme case is when the cold-forming is caused by bending moment (m_ϕ) only. This implies no residual normal force ($n_z \text{ res}$), and no change of thickness (Δt). In this case the radius of neutral surface is the geometric average of the radius of inner and outer surfaces according to *Karren* and *Gohil* /3/. If the cold-forming is caused by bending moment (m_ϕ) only, there will be residual stresses in the length direction, but their resulting force will be zero. The truth is probably somewhere between the extreme cases, which gives the conclusion that there are residual normal forces caused by cold-forming carried out by punching of some kind. The amount of the residual forces depends on the external circumstances during the cold-forming.

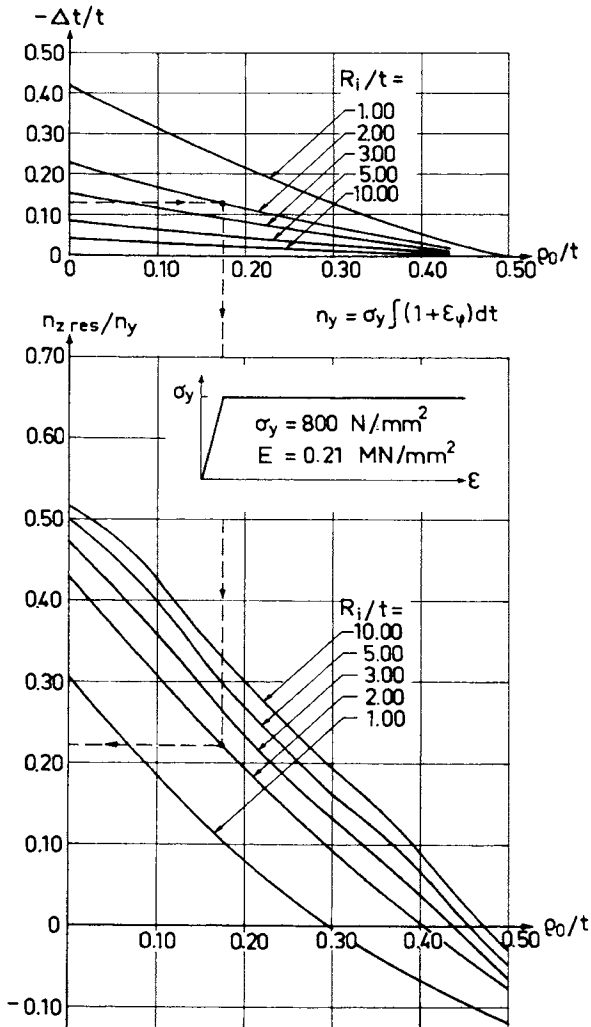


FIGURE 8 Resulting residual force $n_z \text{ res}$ and change in thickness $\Delta t/t$ as function of p_0/t . Steel A.

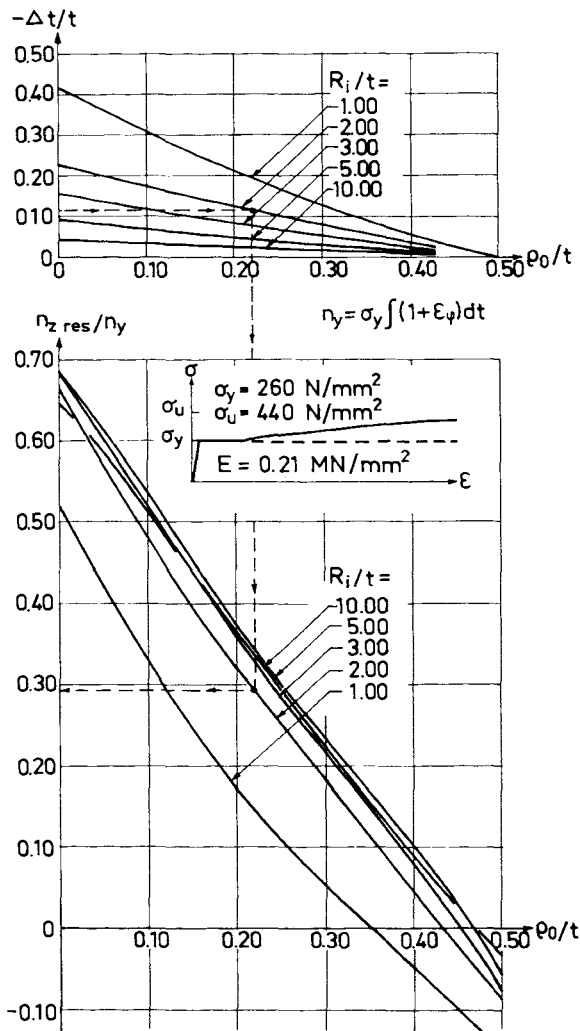


FIGURE 9 Resulting residual force $n_z \text{ res}$ and change in thickness $\Delta t/t$ as function of ρ_0/t . Steel B.

Residual stresses in circular sections have earlier been studied by *Anand and Griffith* /1/, but they have not taken into account the stresses in the length direction (z-direction).

2.2 Experimental investigation

2.2.1 Test specimen

The measurement of residual stresses in channel members has been finished for one specimen with a length of 2050 mm, a width of 250 mm and a height of 125 mm. The cold-formed corners had an inner radius equal to 3.0 times the plate thickness of 7.5 mm. The section of the specimen is illustrated below in FIGURE 12 together with test results.

The test specimen was cold-formed in a press brake by *Gränges Oxelösunds Järnverk AB* which also had manufactured the used steel named "OX 802", which was quenched and tempered in a continuous roller quenching unit. The dimensions of the press brake are shown in FIGURE 10. Maximum pressure force was 1350 kN.

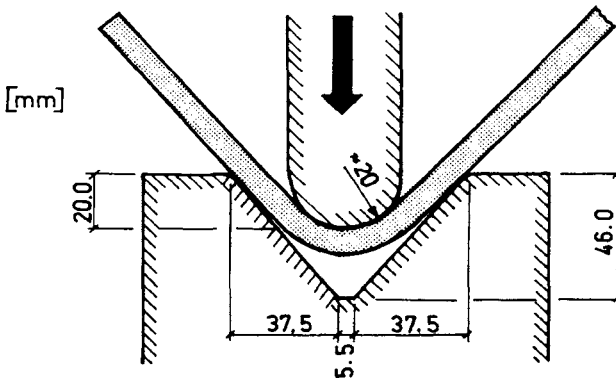


FIGURE 10
Press brake
dimensions.
Final position.

The uniaxial σ - ϵ -relation for the used "OX 802" steel is shown in FIGURE 11. The strain-hardening is neglectible, why the "OX 802" steel has an elastic-plastic behaviour.

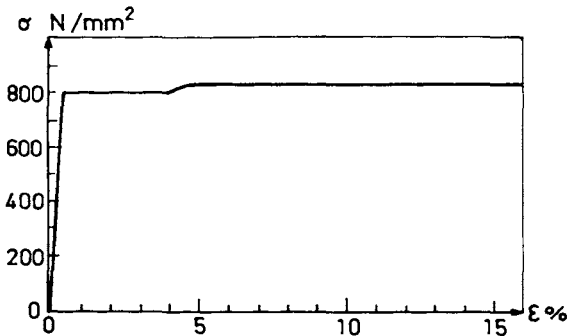


Figure 11
Result from
uniaxial tensile
test of OX 802-
steel.

2.22 Method of residual stress measurement

By cutting up the channel section by sawing at a distance of 800 mm from one end, the residual stresses were released. The corresponding elastic strains were registered by foil strain gages at outer and inner surfaces. Then the residual stresses were calculated by *Hooke's* law. A more detailed description are omitted in this paper. In FIGURE 12 the places of cutting are illustrated.

2.23 Test result

In FIGURE 12 the measured residual stresses σ_z^* are shown. σ_z^* out and σ_z^* in are the stresses at the surfaces registered by strain gages. The release of stresses is equivalent to an elastic unloading of the forces caused by residual stresses, why the measured stresses σ_z^* are

not directly comparable with the theoretical results. If plane sections remain plane the released stress distribution is linear. A more adequate comparison may be made between the average measured stress

$$\sigma_{z\ av}^* = (r_{out} \cdot \sigma_{z\ out}^* + r_i \cdot \sigma_{z\ in}^*) / (r_{out} + r_i) \quad (30)$$

and the theoretical residual force $n_z\ corr.$ For the test specimen the average change in thickness was 3.9 %, which gives $n_z\ corr./n_y = 0.09$. This in comparison with $\sigma_{z\ av}^*/\sigma_y \approx 0.11$ for the test specimen shows that the agreement is acceptable.

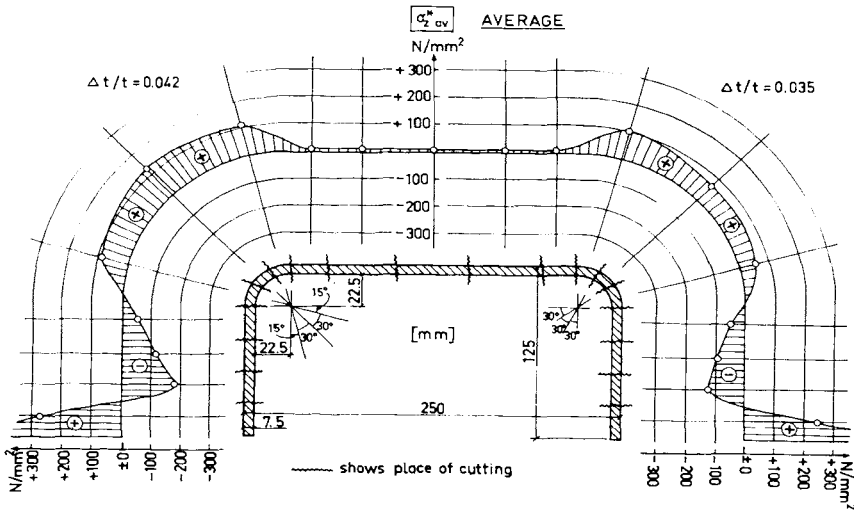


FIGURE 12a Measured residual stresses (average).

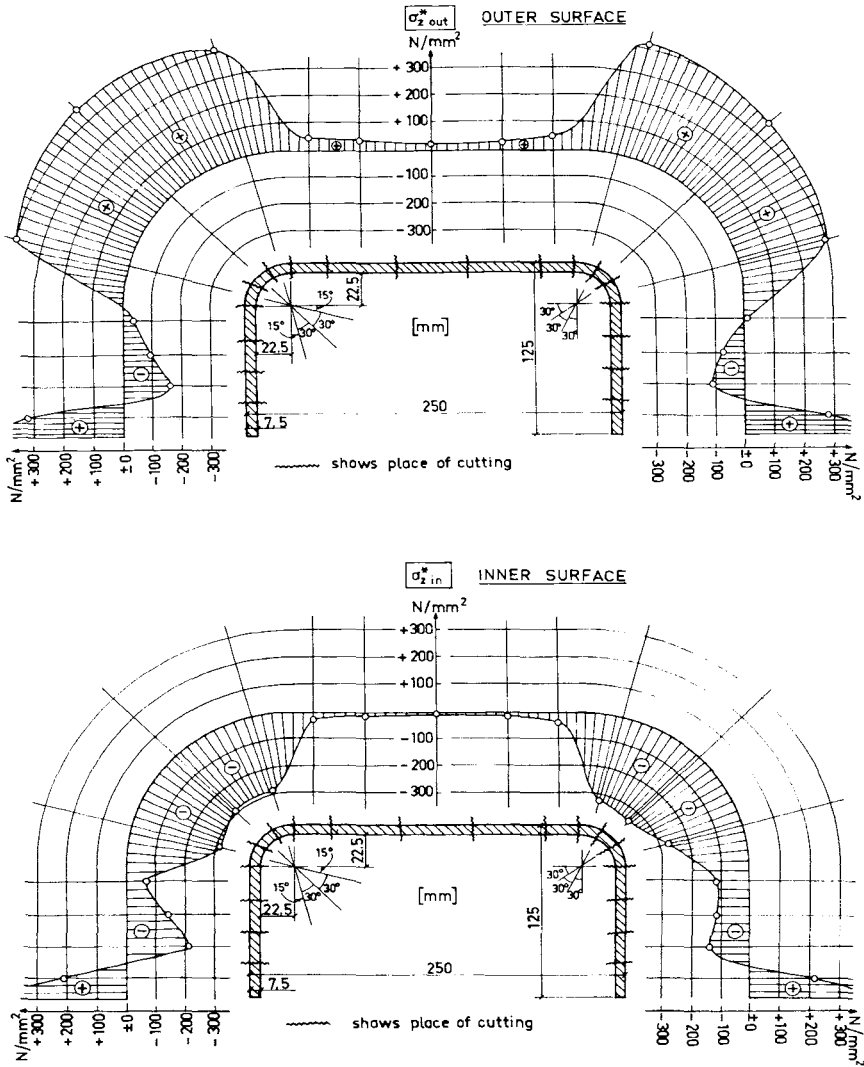


FIGURE 12b Measured residual stresses (surfaces).

3. EFFECT ON BUCKLING STRENGTH OF BOX COLUMNS

3.1 Method of calculation

3.1.1 Box column with welds at corners

Nylander /6/ has developed a method of calculation for plate buckling in overcritical range. This method enables to consider initial (residual) stresses and initial deflections in a relatively simple manner and is shortly described below.

The calculation is based on a simply supported plate, which has been cut out of a square box column (FIGURE 13). The studied plate is separated into two parts, a plate acting only in plate bending and a system of strips 1-7 and 1'-7', taking the membran stresses only. The model is illustrated in FIGURE 13. The strips are connected to the plate at the points A-G and A'-G'. The strip system follows the bending deformation of the plate. The initial stresses are taken into account by the initial forces T_{01} , T_{02} and T_{03} .

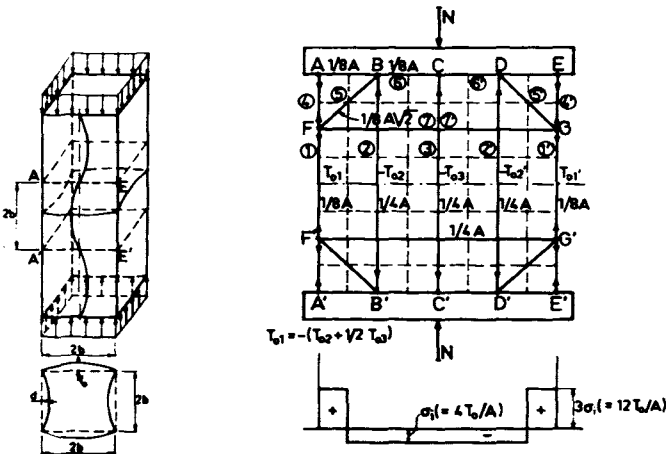


FIGURE 13
(*Nylander /6/*)
Model of calculation.

Instead of trying to get a complex theory for this highly statically indeterminate system in question, the treatment is started from a relatively detailed study of the stresses in different parts of the elastic plate caused by the bending and torsional moments and the normal forces. Then that load has been determined at which total yielding (yield stress over the whole cross section) will occur at the point considered, if moments and normal forces have the values calculated from the theory of elasticity. At the judgement of the failure the following points have been considered.

- 1) The midpoint of strip (1). Yielding due to normal force in the direction of the load N.
- 2) The midpoint of the strip (2). Yielding due to bending moment and normal force in the direction of the load N.
- 3) The centre of the plate (midpoint of strip (3)). Yielding due to bending moment and normal force in the direction of the load N.
- 4) The corner points. Yielding due to torsional moment and normal force in the direction of the load N.

For most of the cases calculated by Nylander the alternatives 2) and 3) above were most dangerous. For high slenderness ratios and small initial stresses the alternative 4) was most dangerous. Of the rather comprehensive results obtained by *Nylander /6/* is in this connection one actual example illustrated in FIGURE 15 below.

3.12 Box column built up by two channel sections welded together

With some modifications of "Nylander's method" the author has made the same calculation for box columns built up by two cold-formed channel members welded together. The inner radius of the corner has been chosen to 3.5 times the plate thickness.

The cold-formed corners cause a restraining, which have been considered by an idealized section without round corners but with some diminished width of the plates. The idealized section has the corners at the shear centres of the cold-formed corners. The corner strip ① (FIGURE 13) is magnified to get agreement with the total area. The most important difference in comparison with corner-welded sections is made by the assumed initial stress distribution (FIGURE 14), which is based on measurements described below in chapter 3.3.

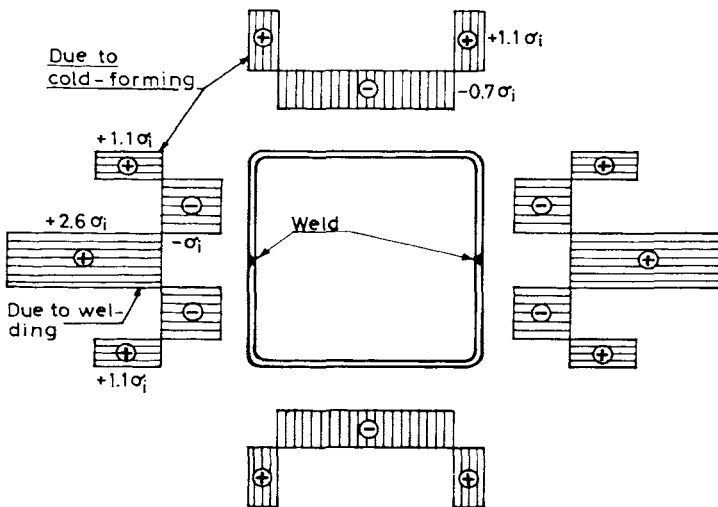


FIGURE 14 Assumed initial stress distribution. Tensile stresses are caused by cold-forming and welding.

Because of the high initial compressive stresses between the weld and the corners, mostly alternative 2) is most dangerous for the welded side. Alternative 4) is most dangerous at high slenderness ratios. However there is still some load capacity if yielding occurs at only two opposite sides of a column. As load capacity criterion for the whole column, the sum of the load capacities for the welded and unwelded sides is chosen.

3.2 Theoretical results

The results of the theoretical treatments described above are shown in FIGURE 15. As comparison results from buckling tests are appended. They are shortly described below in chapter 3.3.

Cold-formed corners seem to have a positive effect on buckling strength in comparison with welded corners. One reason is the more favourable initial stress distribution with tension at corners caused by cold-forming and tension at midpoints of plates caused by welding. Another reason is the less buckling width of the plates. If mild steel is used the strain-hardening caused by cold-forming results in an increase of the yield stress referring to *Yu, Liu and McKinney /9/*. This will also have a positive effect on the load capacity with regard to buckling, when using mild steel.

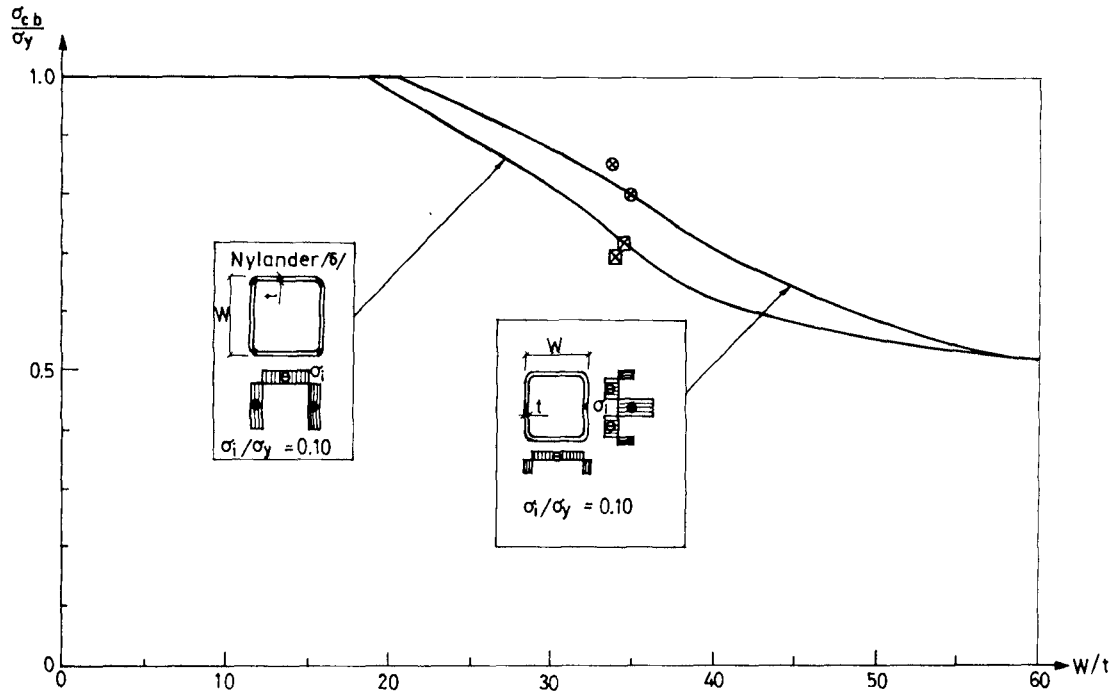


FIGURE 15 Theoretical nominal buckling stresses σ_{cb} when $\sigma_i/\sigma_y = 0.10$.
 Plotted test results. $\sigma_y = 780 \text{ N/mm}^2$, $E = 0.21 \text{ MN/mm}^2$.
 Assumed initial deflection is 1 o/oo of column width.

3.3 Tests

3.31 Test specimens

Four short column tests have been carried out in order to compare the effect of cold-formed corners contrary welded corners. The columns had the same dimensions but the strengths of the welds were varied. The test specimens are presented below in TABLE A. All columns were made of "OX-802" steel described above in chapter 2.21. The welding was made with an half-automatic protective-atmosphere arc welding machine (ESAB A-10, LDA 400) with 80% CO₂ and 20% Ar as inert gas. The welding filler wires used were 1 mm "OK Autrod 1251" and "1312" by ESAB for the "hard" and the "mild" welds, respectively.

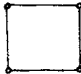
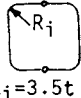
Test no.	Section	Welds	Length ℓ mm	Width W mm	Thickness t mm	W/t
1a		hard	1148	237.0	7.0	33.9
1b		mild	1148	237.7	6.9	34.2
2a		hard	1148	234.2	7.1	32.9
2b		mild	1148	239.0	6.8	35.0

TABLE A Buckling test specimens.

3.32 Residual stresses (initial stresses)

The test specimens were manufactured with the lengths of 2080 mm, which were longer than the column test lengths of 1148 mm. This was done

to enable residual stress measurements at the distance of 3.5 times the column widths from the ends of the manufactured columns. The residual stresses were released by cutting up the specimens by sawing. The released strains at the outer surfaces were registered by foil strain gages. Because of practical difficulties there was no possibility to apply foil strain gages inside the columns. At the department therefore a comprehensive work has been done in developing an equipment which has made it possible to register the changes of curvature released by cutting up the specimens. With the knowledges of the released strains at the outer surfaces and the changes of curvature the residual stresses were calculated for both the outer and the inner surfaces.

A detailed description of the developed equipment for residual stress measurements in box columns is omitted herein but will be published in a near future at the department. In FIGURES 16a and 16b the measured initial stress distributions are shown for one welded and one unwelded side of specimen 2a.

For the other specimens the measured initial stresses are presented below in TABLE B, where σ_{ia} is the average stress for 3/4 of the widths of the column sides. $\Delta\sigma_{ia}$ is the average deviation from σ_{ia} for the outer and inner surfaces. For the midwelded sides of specimens 2a and b σ_{ia} and $\Delta\sigma_{ia}$ are related to the zones between the cold-formed corners and the welds.

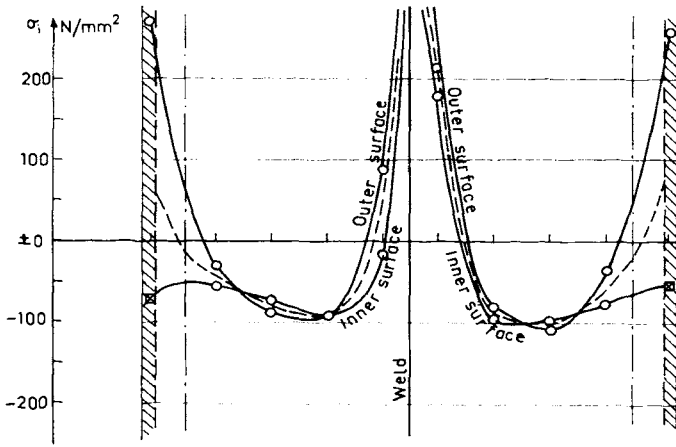


FIGURE 16a Initial stresses σ_i . Cold-formed corners. Welded side. Specimen 2a.

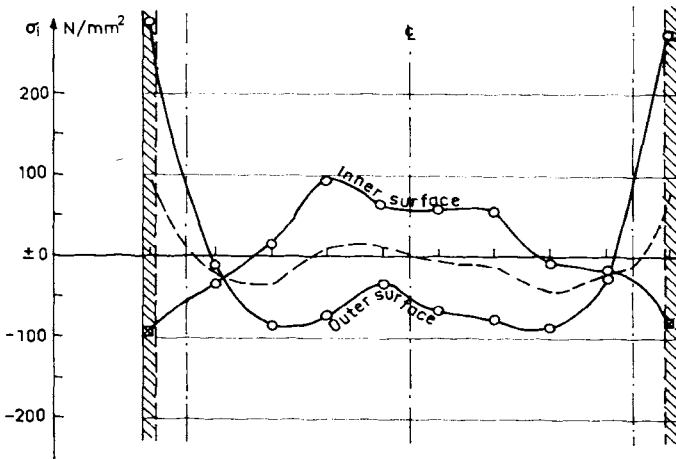


FIGURE 16b Initial stresses σ_i . Cold-formed corners. Unwelded side. Specimen 2a.

Test specimen no.	Weld		σ_{ia} N/mm ²	$\Delta\sigma_{ia}$ N/mm ²
	h="hard"	m="mild"		
1a	h		- 131	\pm 17
			- 78	$\bar{+}$ 30
			- 78	$\bar{+}$ 24
			- 98	$\bar{+}$ 15
1b	m		- 107	\pm 51
			- 52	\pm 6
			- 59	\pm 3
			- 63	$\bar{+}$ 56
2a	h		- 12	$\bar{+}$ 58
		*	- 84	$\bar{+}$ 11
			- 35	\pm 2
		*	- 132	$\bar{+}$ 64
2b	m		- 52	\pm 84
		*	- 44	$\bar{+}$ 8
			- 30	$\bar{+}$ 2
		*	- 10	$\bar{+}$ 87

TABLE B Measured initial stresses for the midzones of the column plates. Values marked *) refers to stresses between corners and midweld.

3.33 Buckling tests

The columns were tested by compressive axial loading with hinge bearings at each end. The results are presented below in TABLE C. Additional they are plotted in FIGURE 15 above. The collapses were caused by local buckling. Overall buckling was not actual because of the short column lengths.

Test specimen no.	Weld h="hard" m="mild"	W/t	σ_y average N/mm ²	σ_{ia}/σ_y average N/mm ²	σ_{cc}/σ_y
1a	h	33.9	800	-0.12	0.695
1b	m	34.2	802	-0.08	0.717
2a	h	32.9	777	-0.08	0.857
2b	m	35.0	780	-0.04	0.801

TABLE C Results of buckling tests, where σ_{cc} is the nominal compressive collapse stress.

According to both theoretical (FIGURE 15) and experimental results (TABLE C) box sections built up by cold-formed channel sections (specimens 2a and 2b) seem to be favourable to the buckling strength compared with box sections with welds at corners (specimens 1a and 1b). Of interest is that "mild" welds are favourable to the buckling strength of corner-welded sections. The mode of action remains the same though there is yielding at corners when using "mild" welds. Furthermore these welds cause less initial stresses, which increases the buckling strength. For the cold-formed sections, in contrary, mild welds are unfavourable, because yielding at the midwelds implies yield hinges. This results in another mode of action, which is unfavourable to the buckling strength.

4. SUMMARY AND CONCLUSIONS

Theoretical analysis according to the theory of plasticity and residual stress measurements indicate that there are residual stresses caused by cold-forming not only in the circumferential direction but also in the length direction of channel members. The amount of the residual

stresses depends on the external circumstances during the cold-forming. Theory and tests show that these residual stresses have a positive effect on the buckling strength of box columns built up by two channel sections welded together in comparison with corner-welded columns.

5. ACKNOWLEDGEMENTS

This investigation at the Dept. of Building Statics and Structural Engineering, The Royal Institute of Technology, Stockholm, Sweden is supported by the National Swedish Council for Building Research. Support is also given by the company Gränges Oxelösunds Järnverk AB, Oxelösund, Sweden for the experimental tests.

6. REFERENCES

- /1/ Anand, S C & Griffith, A R: "Elastic-Plastic Buckling of Cold-Formed Circular Rings", Proceedings of the First Specialty Conference on Cold-Formed Steel Structures, Rolla, Mo., August 19-20, 1971.
- /2/ Karren, K W: "Corner Properties of Cold-Formed Steel Shapes", Journal of the Structural Division, ASCE, Vol. 92, No. ST1, Proc.paper 5112, Feb., 1967, pp. 401-432.
- /3/ Karren, K W & Gohil, M M: "Strain Hardening and Aging in Cold-Formed Steel", Journal of the Structural Division, ASCE, Vol. 101, No. ST1, January, 1975, pp. 187-200.
- /4/ Mendelson, A: "Plasticity: Theory and Application", The MacMillan Company, New York 1968, pp. 123-137, 164-171.
- /5/ von Mises, R: "Mechanik der festen Koerper im plastisch deformablen Zustand", Göttinger Nachr., Math.-Phys. Kl., 1913, pp. 582-592.

- /6/ Nylander, H: "Knäckning och buckling av svetsade lådpelare", Nordiska Forskningsdagar för stålkonstruktioner. Oslo 1973. ("Local and overall buckling of welded box columns", Bulletin no. 110 from the Dept. of Building Statics and Structural Engineering, Royal Inst. of Technology, Stockholm, 1974).
- /7/ Prandtl, L: "Spannungsverteilung in plastischen Koerpern", Proceedings of the 1 st International Congress on Applied Mechanics, Delft, 1924, pp. 43-54.
- /8/ Reuss, E: "Beruecksichtigung der elastischen Formaenderungen in der Plastizitätstheorie", Z. Angew. Math. Mech., 10, 1930, pp. 266-274.
- /9/ Yu, W-W & Liu, V A S & McKinney, W M: "Structural Behavior and Design of Thick, Cold-Formed Steel Members", Proceedings of the Second Specialty Conference on Cold-Formed Steel Structures, Rolla, Mo., October 22-24, 1973.

7. NOTATIONS

The following symbols are used in this paper:

A	= section area
A_c	= area of cold-formed section parts
C	= curvature of inner surface
C_o	= curvature of neutral surface
E	= modulus of elasticity
k	= strain hardening coefficient
m_φ	= loading moment during cold-forming
n	= strain hardening exponent
n_c	= parameter defining increment of curvature

n_t	= parameter defining increment of thickness
n_y	= comparison yield force
$n_z \text{ corr}$	= corrected residual force
$n_z \text{ res}$	= residual force
n_φ	= loading normal force during cold-forming
N	= axial load
r	= radius coordinate
r_i	= radius of inner surface
r_{out}	= radius of outer surface
R_i	= final radius of inner surface
t	= thickness
T_{01}, T_{02}, T_{03}	= initial strip forces
W	= width
z	= length coordinate
Δt	= change in thickness
$\Delta\sigma_{ia}$	= deviation stress for outer and inner surfaces from average initial stress
$\epsilon_\varphi, \epsilon_r, \epsilon_z$	= total strains in polar coordinate directions
$\epsilon_\varphi^e, \epsilon_r^e, \epsilon_z^e$	= elastic strains in polar coordinate directions
$\epsilon_\varphi^p, \epsilon_r^p, \epsilon_z^p$	= plastic strains in polar coordinate directions
ϵ_{et}	= equivalent total strain
ϵ_p	= equivalent plastic strain
ν	= Poisson's ratio
ρ	= internal radius coordinate
ρ_0	= distance between inner and neutral surfaces
ρ_{out}	= distance between inner and outer surfaces
$\sigma_\varphi, \sigma_r, \sigma_z$	= stresses in polar coordinate directions
σ_{cb}	= nominal critical buckling stress (theoretical)

σ_{cc}	= nominal compressive collapse stress (test)
σ_e	= equivalent stress
σ_i	= initial stress
σ_{ia}	= average initial stress
σ_{ri}	= radial pressure at inner surface
σ_y	= yield stress (uniaxial test)
σ_u	= ultimate stress (uniaxial test)
$\sigma_z \text{ corr}$	= corrected residual stress (theory)
$\sigma_z \text{ res}$	= residual stress (theory)
σ_z^*	= residual stress (measured)
$\sigma_z^* \text{ av}$	= average residual stress (measured)
$\sigma_z^* \text{ in}, \sigma_z^* \text{ out}$	= residual stresses (measured) at surfaces
φ	= circumferential coordinate